High-throughput sequencing-based analysis of gene expression of hepatitis B virus infection-associated human hepatocellular carcinoma

HAO ZENG[1*], YING HUI[1*], WENZHOU QIN[2], PEISHENG CHEN[3], LIFANG HUANG[2], WENFU ZHONG[2], LIWEN LIN[2], HUI LV[2] and XUE QIN[4]

Departments of [1]Clinical Laboratory, [2]Pathology and [3]Hepatobiliary Surgery, Guigang City People's Hospital, Guigang, Guangxi 537100; [4]Department of Clinical Laboratory, The First Affiliated Hospital of Guangxi Medical University, Nanning, Guangxi 530021, P.R. China

Received September 24, 2019; Accepted May 13, 2020

DOI: 10.3892/ol.2020.11879

Abstract. Hepatitis B virus (HBV) infection is a critical factor for the initiation and progression of hepatocellular carcinoma (HCC). Gene expression profiles for HBV-associated HCC may provide valuable insight for the diagnosis and treatment of this type of HCC. The present study aimed to screen the differential genes in human HCC tissues based on high-throughput sequencing and to predict the potential therapeutic targets. Total mRNA was extracted from human HCC tissues and paracancerous tissues and sequenced using the Hiseq4000 sequencing platform. Differential gene expressions were screened and further analyzed using quantitative PCR and immunohistochemistry. A total of 2,386 differentially expressed genes were screened. Of these, 1119 were upregulated and 1,267 were downregulated in paracancerous tissues compared with tumor tissues. Gene Ontology term analysis demonstrated that differentially expressed genes were involved in carboxylic acid catabolism, monocarboxylic acid metabolic processes and α-amino acid metabolic processes. Molecular functional analysis revealed that the differentially expressed genes functioned in oxidoreductase activity, for example acting on CH-OH group of donors and permitting identical protein binding, anion binding, coenzyme binding and monocarxylic acid transporter activity. The Kyoto Encyclopedia of Genes and Genomes analysis reported that the differentially expressed genes were primarily concentrated in 20 signaling pathways, such as valine, leucine and leucine degradation, retinol metabolism and the cell cycle. Differential expression of proteins regulating the cell cycle, including stratifin, cyclin B1 and cyclin-dependent kinase 1, were significantly higher in tumor tissue compared with those in paracancerous tissue at both the mRNA and protein levels. These results were consistent with those obtained from high-throughput sequencing, indicating the reliability of the high-throughput sequencing. Together, these results identified differentially expressed genes and predicted the subsequent signaling pathways, which may be involved in the occurrence and development of HCC. Therefore, the present study may provide novel implications in the therapeutic and diagnosis of HCC.

Correspondence to: Dr Ying Hui, Department of Clinical Laboratory, Guigang City People's Hospital, 1 Zhongshan Middle Road, Guigang, Guangxi 537100, P.R. China
E-mail: hunyin112@163.com

Dr Xue Qin, Department of Clinical Laboratory, The First Affiliated Hospital of Guangxi Medical University, 6 Shuangyong Road, Qingxiu, Nanning, Guangxi 530021, P.R. China
E-mail: qin333x@163.com

*Contributed equally

Key words: high-throughput sequencing, hepatocellular carcinoma, mRNA

Introduction

Hepatocellular carcinoma (HCC) is the most common type of primary hepatocellular carcinoma, accounting for 90% of primary hepatocellular carcinoma cases, and is the leading cause of cancer-associated death worldwide (1). Globally, ~350 million people are infected with hepatitis B virus (HBV), and HBV infection accounts for at least 50% of HCC cases (2). HBV-associated HCC is therefore frequently observed. Notable progress has been made in the diagnosis and treatment of HCC, and overall treatment efficacy has been improved, especially following the development of multi-modality therapy, such as hepatectomy, minimally invasive treatment and liver transplantation (3). However, most patients with HCC are diagnosed during the middle and advanced stages, during which traditional radiotherapy and chemotherapy have limited clinical benefit. This is primarily due to high rates of recurrence and metastasis (4), therefore, it is important to identify novel diagnostic and prognostic markers to aid earlier intervention.

The occurrence and development of HCC are caused by genetic and epigenetic variations, including gene mutations, copy number variations and abnormal methylation (5).

High-throughput technology has identified a large number of tumor driver gene mutations and epigenetic alterations associated with the pathogenesis of HCC (6-10), which may have potential as diagnostic and prognostic molecular markers (11,12). Mutations in key driver genes lead to uncontrolled proliferation and clonal amplification of cancer cells (13-15). However, differentially expressed genes in HCC have not been screened and the subsequent signaling pathways involved in the development of HCC have not been validated.

The present study aimed to identify potentially novel therapeutic targets for HCC using high-throughput-based gene expression analysis in human HCC tissues. To prevent false-positive results from high-throughput screening, immunohistochemical analysis was also performed to verify differential gene expression.

Materials and methods

Tissue collection. The samples were collected from eight patients with HBV-associated HCC at the Department of Hepatobiliary Gland Extracorporeal Surgery of Guigang People's Hospital (Guigang, China) between January 2017 and March 2017. The age of the patients ranged from 38 to 61 years (median age, 48.5 years; male: Female ratio of 5:3), and the primary HCC tissue specimens and matched paracancerous liver tissues were collected during hepatectomy. Clinicopathological characteristics of patients, including age and serum levels of bilirubin, alkaline phosphatase, albumin, alanine transaminase (ALT), aspartate transaminase (AST), alphafetoprotein (AFP), hepatitis B surface antigen (HBsAg), hepatitis B surface antibody (HBsAb), hepatitis B e antigen (HBeAg), hepatitis B e antibody (HBeAb) and hepatitis B core antibody (HBcAb) were collected. HCC was confirmed by a pathological report from Guigang People's Hospital based on the evaluation of differentiation and metastasis as previously described (16). The tissues were divided into two groups: Paracancerous tissue group and hepatocellular carcinoma tissue group. The inclusion criteria were as follows: i) No etiological evidence of hepatitis C virus, type 2 diabetes mellitus, fatty liver, alcoholic liver or aflatoxin exposure history; ii) no preoperative radiotherapy, digital subtraction angiography intervention, antineoplastic drug therapy or and radiofrequency ablation; and iii) no other history of cancer. Patients who did not meet one of the aforementioned criteria were excluded. Three tumor tissues and corresponding paracancerous tissues were analyzed using high-throughput sequencing. Three differentially expressed genes, stratifin *(SFN)*, cyclin B1 *(CCNB1)* and cyclin-dependent kinase 1 *(CDK1)* were verified in the total 8 tumor tissues and corresponding paracancerous tissues.

After the specimens were removed, tumors and paracancerous liver tissues were cut into small pieces (~2 mm) on ice, then put into 1.5 ml nucleic acid-free centrifugal tubes and stored in liquid nitrogen. Cancer tissues and paracancerous tissues were collected from the non-necrotic area of the cancer, and paracancerous liver tissues were taken from the non-invasive area 2 cm away from the edge of the obvious mass, avoiding the burning site of the scalpel and preventing the loss of DNA and RNA due to high temperature. Patients provided informed written consent before organizing the collection, and the study was approved by the Ethics Committee of Guigang City People's Hospital.

Construction of the Illumina sequencing library. Total RNA was extracted from the samples using TRIzol® (Invitrogen; Thermo Fisher Scientific, Inc.). The concentration and purity of the RNA were detected using Nanodrop 2000 (Thermo Fisher Scientific, Inc.), the integrity of RNA was detected by agarose gel electrophoresis (0.5% gel; ethidium bromide staining and visualization at UV light), and the value of RNA integrity was determined using Agilent 2100 (Agilent Technologies, Inc.). The total amount of RNA required for single library construction was >5 μg, the concentration was >200 ng/μl, and optical density 260/280 was between 1.8 and 2.2. Then, a Ribo-Zero Magnetic kit (Epicentre; Illumina, Inc.) was used to remove ribosomal RNA, RNase R (Epicentre; Illumina, Inc.) was used to remove linear RNA and a TruSeq™ Stranded Total RNA Library Prep kit (Illumina, Inc.) was used to construct Paired-End sequencing library. The analysis of mRNA was performed using the Hiseq4000 sequencing platform (Illumina, Inc.). Principal component analysis (PCA) was used to analyze multidimensional data.

Sequencing data analysis. SepPrep and Silkle software (linux-64 v1.3.2; Anaconda Clound) were used to examine the data quality and the data obtained after quality control (Phred quality score) with the reference genome data were compared using Bowtie version 2. KNIEF and CIRCexplorer2 were used to predict the expression of RNA, and then levels of RNA in the samples were calculated.

Differentially expressed gene enrichment analysis. Gene Ontology software was used for enrichment analysis of GO functions, including molecular function, cell components, and biological processes, and Kyoto Encyclopedia of Genes and Genomes (KEGG) pathway enrichment analysis was carried out using the KEGG Orthology-Based Annotation System and KEGG annotation (https://www.genome.jp/kegg-bin/get_htext?ko00001).

Prediction of target genes. Differential analysis of gene expression was performed using DESeq version 2 (Bioconductor) to predict target genes of RNA.

Quantitative (q)PCR. According to the results of high-throughput sequencing, three differentially expressed RNAs (*SFN*, *CCNB1* and *CDK1*) were analyzed using fluorescence qPCR. The primer sequences used are listed in Table I. Total mRNA was amplified using a one-step RT-PCR kit (00081405, CWBio). The primers were added into a 25-μl ULtraSYBR mixture (01170, CWBio) PCR reaction system according to the manufacturer's protocol. The thermocycling conditions were as follows: Pre-denaturation at 95˚C for 10 min, 95˚C denaturation for 10 sec, 58.5˚C annealing for 30 sec and 72˚C extension for 30 sec (40 cycles). The Cq value for each gene was determined and expression levels of target genes were calculated using the $2^{-\Delta\Delta Cq}$ method (17). mRNA expression of target genes were normalized to *GAPDH*.

Immunohistochemistry. Cancer tissues were fixed with 4% paraformaldehyde overnight at 4˚C. The tissues were then dehydrated using 70, 80 and 90% ethanol, and mixed with anhydrous ethanol and xylene for 15 min, xylene I for 15 min and

Table I. Primer sequences.

Genes	Primers, 5'-3'	Primer length, bp	Product length, bp	Annealing, ˚C
SFN			116	61.4
Forward	GGTGACTACTACCGCTACCTGG	22		
Reverse	GGCATCTCCTTCTTGCTGACG	21		
CCNB1			157	56.9
Forward	TTGAGGAAGAGCAAGCAGTC	20		
Reverse	AACCGATCAATAATGGAGACAG	22		
CDK1			110	57.5
Forward	AGGATGTGCTTATGCAGGATTC	22		
Reverse	CATGTACTGACCAGGAGGG	19		
GAPDH			106	57.2
Forward	CAATGACCCCTTCATTGACC	20		
Reverse	GAGAAGCTTCCCGTTCTCAG	20		

Table II. Quality analysis of the original data.

Sample	Reads no.	Bases, bp	Q30, bp	N, %	Q20, %	Q30, %
Control 1	43,704,194	6,599,333,294	6,226,745,352	0.001709	97.73	94.35
Control 2	41,440,988	6,257,589,188	5,914,658,053	0.001422	97.81	94.51
Control 3	42,235,972	6,377,631,772	6,099,059,319	0.001376	98.28	95.63
Cancer 1	40,926,974	6,179,973,074	5,744,415,761	0.000725	97.11	92.95
Cancer 2	44,150,718	6,666,758,418	6,218,604,371	0.001765	97.24	93.27
Cancer 3	42,218,858	6,375,047,558	5,979,826,518	0.001859	97.5	93.82

Controls 1, 2 and 3 were the paracancerous liver tissues of cancer samples 1, 2 and 3, respectively.

xylene II for 15 min (until transparent). Tissues were embedded in paraffin and sliced into 10-μm sections. The paraffin slices were dewaxed and hydrated in 70, 75, 80, 85 and 95% alcohol. Then, 3% (v/v) H_2O_2 was used to block endogenous peroxidase activity for 5 min at room temperature. Immunostaining of the slides was performed using the following antibodies overnight at 4˚C: Rabbit polyclonal anti-SFN (1:50, bs-20373R, BIOSS), rabbit polyclonal anti-CCNB1 (1:400, bs-20373R, BIOSS) and rabbit polyclonal anti-CDK1 (1:100, bs-20373R, BIOSS). The slides were then washed with PBS and incubated with horseradish peroxidase-labeled goat anti-rabbit IgG secondary antibody (1:10,000; A16104SAMPLE; Thermo Fisher Scientific, Inc.) for 30 min at room temperature, and visualized with 3,3'-diaminobenzidine chromogen for 3 min at room temperature. At least four fields were taken from each image using a light microscope (magnification, x200; BX51, Olympus Corporation). Staining intensity was analyzed by Image-Pro Plus software (National Institutes of Health). The relative expressions of target proteins were normalized to the negative control (without primary antibody).

Statistical analysis. All data were analyzed using SPSS version 19.0 (IBM Corp.) The differences between groups were analyzed using unpaired Student's t-tests and $P<0.05$ was considered to indicate a statistically significant difference.

Results

Basic information of the patients. Eight patients with HCC were enrolled in the present study. The age of the patients ranged from 38 to 61 years. The mean values of bilirubin, alkaline phosphatase, albumin, ALT, AST and AFP serum levels were 15.0 μM, 92.1 U/l, 44.6 g/l, 31.5 U/l, 33.6 U/l and 785.3 ng/ml, respectively. HBsAg, HBeAb and HBcAb were positive in all patients . The patients were in a stage of medium- and low-differentiation without lymph node involvement and distal metastasis. All patients were diagnosed with cirrhosis and portal vein embolism, but without ascites (data not shown).

Quality analysis of the data. The quality of the data is presented in Table II. The sequence numbers obtained in paracancerous tissues and cancer tissues were 43,704,194, 41,440,988, 42,235,972 and 4,092,974, 44,150,718 and 42,218,858, respectively. Phred bases with a value >20 accounted for 97% of the total number of bases, indicating that the original sequencing data were of good quality and could be used for subsequent data analysis.

Quality control analysis of sequencing data. The data quality control analysis showed that the total number of reference

Table III. Statistical analysis of RNASeq map.

Sample	Clean_Reads	Total_Mapped, n (%)	Multiple_Mapped, n (%)	Uniquely_Mapped, n (%)
Control 1	43,594,562	40,504,709 (92.91)	2,163,607 (5.34)	38,341,102 (94.66)
Control 2	41,339,382	38,683,072 (93.57)	1,788,575 (4.62)	36,894,497 (95.38)
Control 3	42,162,810	39,597,473 (93.92)	1,290,633 (3.26)	38,306,840 (96.74)
Cancer 1	40,695,892	37,637,436 (92.48)	1,630,956 (4.33)	36,006,480 (95.67)
Cancer 2	44,010,224	40,362,249 (91.71)	4,109,173 (10.18)	36,253,076 (89.82)
Cancer 3	42,106,446	38,830,579 (92.22)	4,455,543 (11.47)	34,375,036 (88.53)

Controls 1, 2 and 3 were the paracancerous liver tissues of cancer samples 1, 2 and 3, respectively.

genome sequences was >90% (Table III), indicating that the quality control of sequencing data was good and could be used in subsequent data analysis.

PCA analysis. PCA analysis showed that there were obvious differences between the control group and cancer group. By contrast, there was no inner difference among the data in each group. Thus, the data could be used in the subsequent analysis (Fig. 1).

Differential gene expression analysis. Differential gene expression analysis is presented in Fig. 2. 2,386 differentially expressed genes were screened (multiple of differentially expressed genes between samples was >1, and the value of differentially expressed genes in samples was <0.05). There were 1119 downregulated and 1,267 upregulated genes in cancer tissues compared with paracancerous tissues.

GO functional enrichment analysis. GO functional enrichment analysis of differentially expressed genes was used to identify GO functional items. Firstly, all genes were mapped to each term in GO database and the number of differentially expressed genes was calculated. Then, significantly enriched differentially expressed genes with the whole genome were analyzed. The GO analysis showed that differentially expressed genes were enriched in the following GO molecular functions: GO: 0046395 carboxylic acid catabolic process, GO: 0032787 monocarboxylic acid metabolic process and GO: 1901605 α-amino acid metabolic processes. Genes were also enriched in the following cellular component functions: GO: 0070062 extracellular exosome, GO: 0044444 cytoplasmic part and GO: 0044459 plasma membrane part. Differentially expressed genes were enriched in the following biological processes: GO: 0016614 oxidoreductase activity, acting on CH-OH group of donors, GO: 0042802 identical protein binding, GO: 0043168 anion binding, GO: 0050662 coenzyme binding and GO: 0008028 monocarboxylic acid transmembrane transporter activity (data not shown).

Enrichment analysis of KEGG signaling pathways of differentially expressed genes. Enrichment analysis of KEGG signaling pathways of differentially expressed genes was based on the whole genome and is shown in Fig. 3. The metabolic pathways and signaling pathways in which differentially expressed genes functioned were determined. The results showed that the differentially expressed genes were mainly concentrated in 20 signaling pathways, including degradation of valine, leucine and isoleucine, retinol metabolism and the cell cycle.

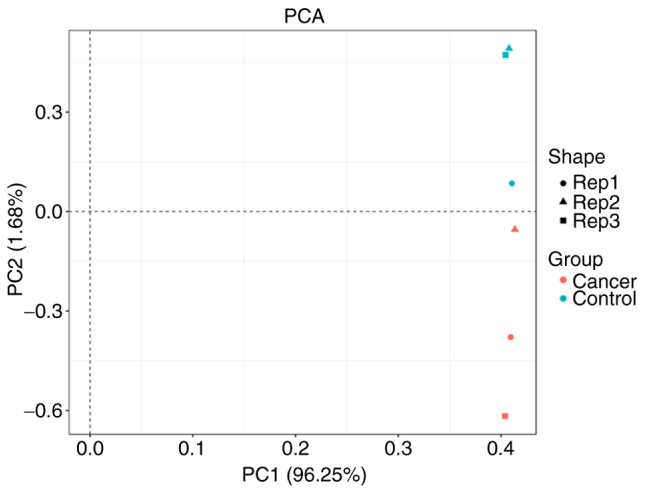

Figure 1. Principal component analysis. Rep1, 2 and 3 corresponded to the sample 1, 2 and 3. PC1 and PC2 represented principal components 1 and 2.

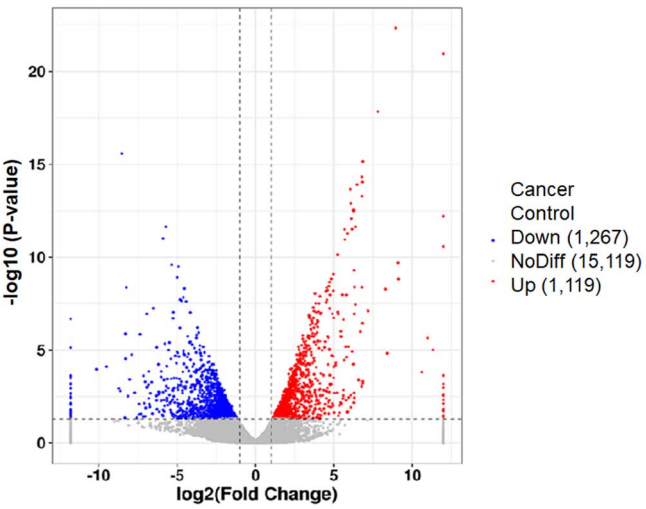

Figure 2. Volcano map of differentially expressed genes. Blue represents downregulated genes and red represents upregulated genes. NoDiff, no difference.

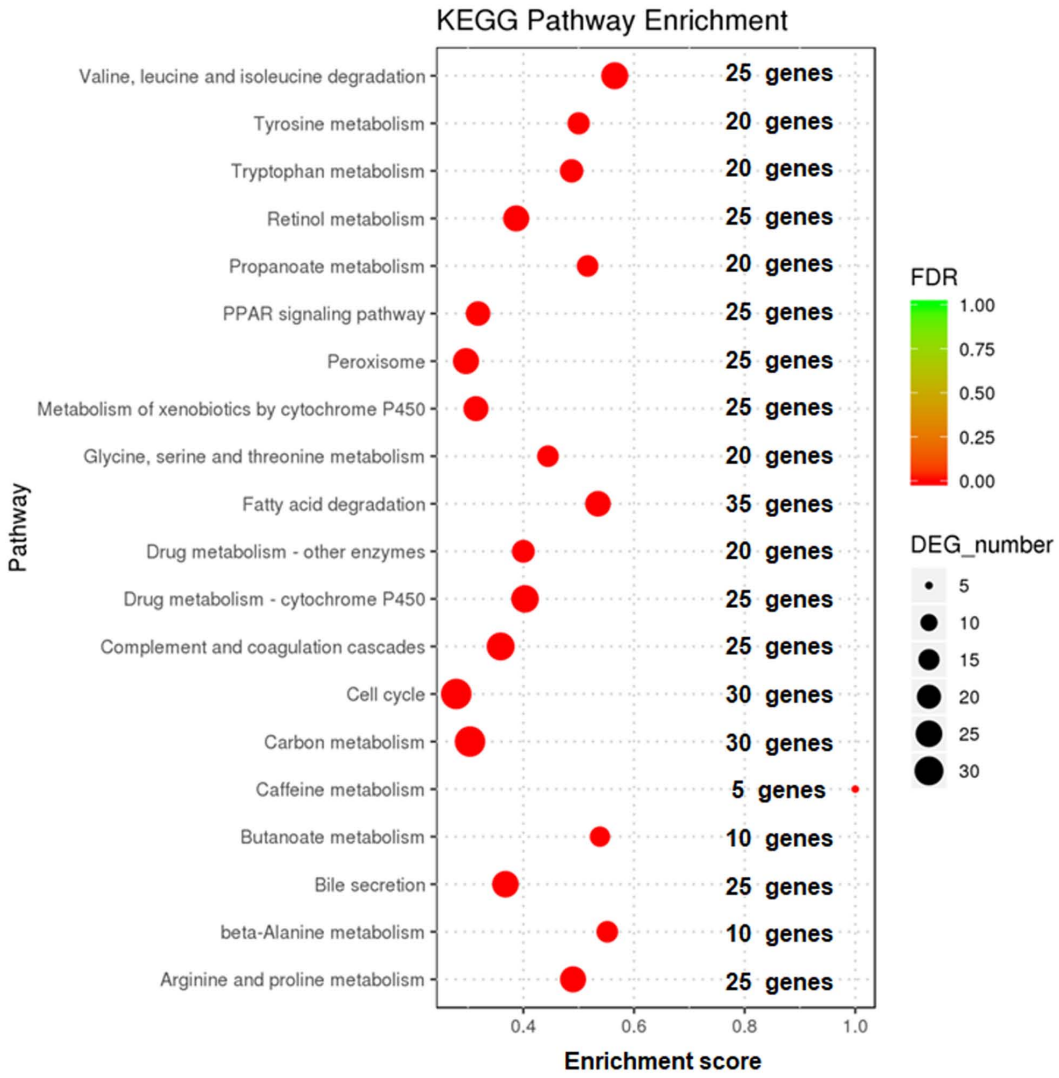

Figure 3. Enrichment analysis of KEGG signaling pathway of differentially expressed genes. The vertical coordinate is the KEGG pathway entry, and the horizontal coordinate is the ratio of the number of differential genes enriched in the pathway to the number of genes annotated in the pathway. The size of the dots in the graph indicates the number of differential genes enriched in the pathway and the number of genes annotated in the pathway. The color indicates the significant P-value of the pathway. KEGG, Kyoto Encyclopedia of Genes and Genomes; FDR, false discovery rate; DEG, differentially expressed gene.

Validation of differentially expressed genes. The validation of three differentially expressed genes is shown in Fig. 4. The results showed that the expression of *SFN*, *CCNB1* and *CDK1* genes in tumors were upregulated in cancer tissues compared with control ($P<0.05$; Figs. 4A and B, S1), which was consistent with the results of high-throughput sequencing. The results were further confirmed using qPCR and a consistent result was obtained (vs. control; $P<0.05$; Fig. 4C).

Discussion

In the present study, differential gene expression between HCC and paracancerous tissues was analyzed. The differentially expressed genes were mainly concentrated in 20 signaling pathways, such as valine, leucine and isoleucine degradation, retinol metabolism and the cell cycle. It was then further confirmed that cell cycle-associated genes (*SFN*, *CCNB1* and *CDK1*) were abnormally expressed in HCC tissues. The present study may provide novel therapeutic targets for HCC.

Due to the lack of early diagnostic measures, the incidence of recurrence and metastasis after operation in HCC is high, and drug treatments have limited therapeutic benefit (18,19). Therefore, early diagnosis and prediction are important to improve the treatment of HCC. Similar to other malignant tumors, HCC is often caused by the activation of oncogenes (*myc*, *ras*) or the inactivation of tumor suppressor genes (e.g., *p53*) (20,21). The aim of the present study was to detect differentially expressed genes in HCC and paracancerous tissues using high-throughput sequencing.

Tumor development is usually associated with multiple signaling pathways (22). KEGG analysis showed that the differentially expressed genes were mainly concentrated in 20 signaling pathways, such as valine, leucine and isoleucine degradation, retinol metabolism and the cell cycle. In addition, 2,386 differentially expressed genes were screened. The differentially expressed genes of *SFN*, *CCNB1* and *CDK1* were selected from the high throughput results for further verification. *SFN, CCNB1* and *CDK1* genes expressed differently in high-throughput results, were associated to the cell cycle (23).

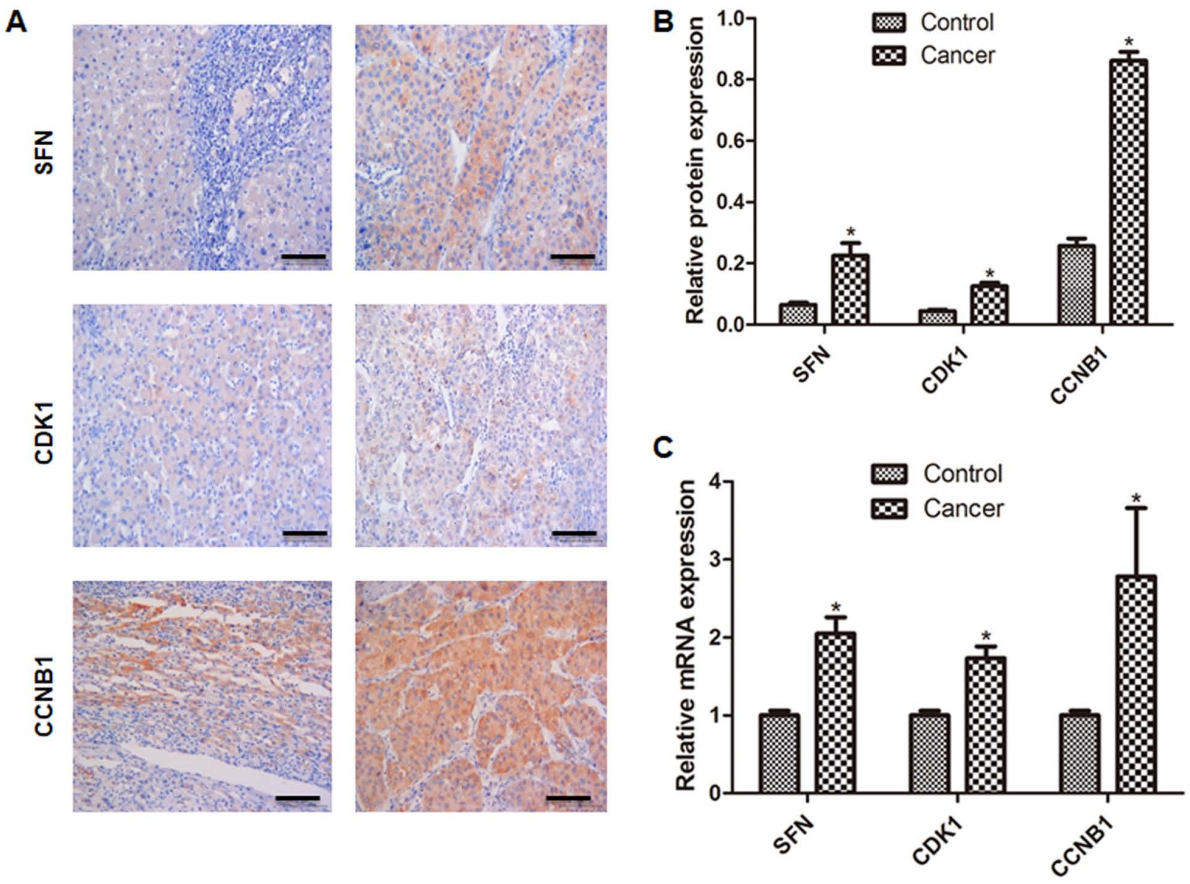

Figure 4. Validation of differentially expressed genes. (A) Representative images of immunohistochemistry from one patient. Control was the paracancerous liver tissue and cancer was the cancer tissue. Scale bar, 100 μm. (B) Quantification of protein expression levels. (C) Quantification of mRNA levels. *P<0.05 vs. respective control. SFN, sulforaphane; CDK1, cyclin-dependent kinase 1; CCNB1, cyclin B1.

Experiments have shown that knocking out the *SFN* gene can lead to cell failure to maintain stable G_2/M cycle after DNA damage and sensitizes cells to DNA damage. This method is therefore used in the treatment of neuroblastic tumor (24). SFN can arrest cell cycle and induce apoptosis of human tumor cells (25). Increased expression of SFN results in the chelation of CDK1/cyclinB1 in cytoplasm, thus blocking the interaction between cell division cycle 2 (*CDC2)* gene and CDK1 and preventing cells from entering into cell mitosis (26-28).

CDK1 is a member of the protein kinase family and is encoded by the *CDC2* gene. At the late stage of G_2, CDK1 and cyclin B1 lotus root synthesize complex, forming mitotic promoter factor, which can promote cell cycling from G_2 to M (29). CDK1 is an important regulator of mitotic initiation, cell cycling and metastasis. High expression of active CDK1 promotes G_2/M expression and accelerates cancer cell growth (30). Some studies have shown that specific inhibitors of CDK1 can induce reversible dormancy of human cells in G_2/M phase, leading to the apoptosis of cancer cells, suggesting that selective inhibitors of CDK1 may play a pivotal role in the treatment of cancer (30,31).

CCNB1 is an important regulator of the cell cycle associated with the detection point of G_2/M phase. Interaction of CCNB1 and CDK1 phosphorylates the substrate cell division homologous protein cyclin 25, initiates cell cycle progression from G_1/S phase to G_2/M phase and promotes mitosis (32). A previous study reported that the abnormal expression of CCNB1 is associated with abnormal cell proliferation and tumorigenesis (33). A number of studies have shown that CCNB1 is highly expressed in breast, lung and gastrointestinal cancer (34-36). In the present study, the results of qPCR and immunohistochemistry demonstrated that the expression of *SFN*, *CCNB1* and *CDK1* was elevated in cancer tissues and that these results were consistent with the high-throughput results.

There were still limitations of the present study. First, only three tumor tissues and corresponding paracancerous tissues were analyzed using high-throughput sequencing. Three differentially expressed genes, *SFN*, *CCNB1* and *CDK1* were verified in the total 8 tumor tissues and corresponding paracancerous tissues. Consistent results were obtained from high-throughput sequencing, PCR and western blotting; however, the differentially expressed genes and their proteins need external validation in a larger cohort of patients with cirrhosis and different stages of HCC. Second, although differentially expressed genes in HCC were screened, the potential value of these genes in the treatment and prognosis of HCC were not confirmed. Third, there were still some discrepancies regarding the differentially expressed genes reported in the present study and previous studies. These might be caused by different patient ethnicities, types of HCC and disease stages. However, larger sample size is crucial and laboratory experiments should be carried out to validate these findings and disclose potential mechanisms.

In conclusion, differentially expressed genes were screened using high-throughput technology and enriched in tumor-associated signaling pathways and functions. The next step is to investigate the functions of these differentially expressed genes.

Acknowledgements

Not applicable.

Funding

Construction Funding of Key Clinical Specialties Guangxi Zhuang Autonomous Region (Z20190320).

Availability of data and materials

The datasets used and/or analyzed during the current study are available from the corresponding author upon reasonable request.

Authors' contributions

HZ, YH, WQ, PC, LH, WZ, LL and HL performed the experiments and analyzed the data. HZ and XQ designed the study and wrote the manuscript. All authors read and approved the final manuscript.

Ethics approval and consent to participate

All patients provided informed written consent before tissue collection, and the study was approved by the Ethics Committee of Guigang City People's Hospital (approval no. 013142017).

Patient consent for publication

Not applicable.

Competing interests

The authors declare that they have no competing interests.

References

1. Yang X, Zhang D, Liu S, Li X, Hu W and Han C: KLF4 suppresses the migration of hepatocellular carcinoma by transcriptionally upregulating monoglyceride lipase. Am J Cancer Res 8: 1019-1029, 2018.
2. Xie Y: Hepatitis B virus-associated hepatocellular carcinoma. Adv Exp Med Biol 1018: 11-21, 2017.
3. Xing H, Qiu H, Ding X, Han J, Li Z, Wu H, Yan C, Li H, Han R, Zhang H, *et al*: Clinical performance of alpha-L-fucosidase for early detection of hepatocellular carcinoma. Biomark Med 13: 545-555, 2019.
4. Jiao D, Li Y, Yang F, Han D, Wu J, Shi S, Tian F, Guo Z, Xi W, Li G, *et al*: Expression of prostate-specific membrane antigen in tumor-associated vasculature predicts poor prognosis in hepatocellular carcinoma. Clin Transl Gastroenterol: May 15, 2019 doi: 10.14309/ctg.0000000000000041 (Online ahead of print).
5. Xiao Z, Yan Y, Zhou Q, Liu H, Huang P, Zhou Q, Lai C, Zhang J, Wang J and Mao K: Development and external validation of prognostic nomograms in hepatocellular carcinoma patients: A population based study. Cancer Manag Res 11: 2691-2708, 2019.
6. Koboldt DC, Zhang Q, Larson DE, Shen D, McLellan MD, Lin L, Miller CA, Mardis ER, Ding L and Wilson RK: VarScan 2: Somatic mutation and copy number alteration discovery in cancer by exome sequencing. Genome Res 22: 568-576, 2012.
7. Ziats MN and Rennert OM: Identification of differentially expressed microRNAs across the developing human brain. Mol Psychiatry 19: 848-852, 2014.
8. Tang ZY, Ye SL, Liu YK, Qin LX, Sun HC, Ye QH, Wang L, Zhou J, Qiu SJ, Li Y, *et al*: A decade's studies on metastasis of hepatocellular carcinoma. J Cancer Res Clin Oncol 130: 187-196, 2004.
9. Sells MA, Chen ML and Acs G: Production of hepatitis B virus particles in Hep G2 cells transfected with cloned hepatitis B virus DNA. Proc Natl Acad Sci USA 84: 1005-1009, 1987.
10. Nakabayashi H, Taketa K, Miyano K, Yamane T and Sato J: Growth of human hepatoma cells lines with differentiated functions in chemically defined medium. Cancer Res 42: 3858-3863, 1982.
11. Schulze K, Nault JC and Villanueva A: Genetic profiling of hepatocellular carcinoma using next-generation sequencing. J Hepatol 65: 1031-1042, 2016.
12. Jin Y, Lee WY, Toh ST, Tennakoon C, Toh HC, Chow PK, Chung AY, Chong SS, Ooi LL, Sung WK and Lee CG: Comprehensive analysis of transcriptome profiles in hepatocellular carcinoma. J Transl Med 17: 273, 2019.
13. Tian J, Tang ZY, Ye SL, Liu YK, Lin ZY, Chen J and Xue Q: New human hepatocellular carcinoma (HCC) cell line with highly metastatic potential (MHCC97) and its expressions of the factors associated with metastasis. Br J Cancer 81: 814-821, 1999.
14. Li Y, Tang ZY, Ye SL, Liu YK, Chen J, Xue Q, Chen J, Gao DM and Bao WH: Establishment of cell clones with different metastatic potential from the metastatic hepatocellular carcinoma cell line MHCC97. World J Gastroenterol 7: 630-636, 2001.
15. Kan Z, Zheng H, Liu X, Li S, Barber TD, Gong Z, Gao H, Hao K, Willard MD, Xu J, *et al*: Whole-genome sequencing identifies recurrent mutations in hepatocellular carcinoma. Genome Res 23: 1422-1433, 2013.
16. Chen D, Li Z, Song Q, Qian L, Xie B and Zhu J: Clinicopathological features and differential diagnosis of hepatocellular carcinoma in extrahepatic metastases. Medicine (Baltimore) 97: e13356, 2018.
17. Livak KJ and Schmittgen TD: Analysis of relative gene expression data using real-time quantitative PCR and the 2(-Delta Delta C(T)) method. Methods 25: 402-408, 2001.
18. He ZX, Xiang P, Gong JP, Cheng NS and Zhang W: Radiofrequency ablation versus resection for Barcelona clinic liver cancer very early/early stage hepatocellular carcinoma: A systematic review. Ther Clin Risk Manag 12: 295-303, 2016.
19. Tejeda-Maldonado J, García-Juárez I, Aguirre-Valadez J, González-Aguirre A, Vilatobá-Chapa M, Armengol-Alonso A, Escobar-Penagos F, Torre A, Sánchez-Ávila JF and Carrillo-Pérez DL: Diagnosis and treatment of hepatocellular carcinoma: An update. World J Hepatol 7: 362-376, 2015.
20. Khordadmehr M, Jigari-Asl F, Ezzati H, Shahbazi R, Sadreddini S, Safaei S and Baradaran B: A comprehensive review on miR-451: A promising cancer biomarker with therapeutic potential. J Cell Physiol 234: 21716-21731, 2019.
21. Mirza AZ: Advancement in the development of heterocyclic nucleosides for the treatment of cancer-A review. Nucleosides Nucleotides Nucleic Acids 38: 836-857, 2019.
22. Nwabo Kamdje AH, Takam Kamga P, Tagne Simo R, Vecchio L, Seke Etet PF, Muller JM, Bassi G, Lukong E, Kumar Goel R, Mbo Amvene J and Krampera M: Developmental pathways associated with cancer metastasis: Notch, Wnt, and Hedgehog. Cancer Biol Med 14: 109-120, 2017.
23. Diaz-Moralli S, Tarrado-Castellarnau M, Miranda A and Cascante M: Targeting cell cycle regulation in cancer therapy. Pharmacol Ther 138: 255-271, 2013.
24. Banelli B, Bonassi S, Casciano I, Mazzocco K, Di Vinci A, Scaruffi P, Brigati C, Allemanni G, Borzì L, Tonini GP and Romani M: Outcome prediction and risk assessment by quantitative pyrosequencing methylation analysis of the SFN gene in advanced stage, high-risk, neuroblastic tumor patients. Int J Cancer 126: 656-668, 2010.
25. Clarke JD, Dashwood RH and Ho E: Multi-targeted prevention of cancer by sulforaphane. Cancer Lett 269: 291-304, 2008.
26. Singh SV, Herman-Antosiewicz A, Singh AV, Lew KL, Srivastava SK, Kamath R, Brown KD, Zhang L and Baskaran R: Sulforaphane-induced G2/M phase cell cycle arrest involves checkpoint kinase 2-mediated phosphorylation of cell division cycle 25C. J Biol Chem 279: 25813-25822, 2004.
27. Steiner M, Clark B, Tang JZ, Zhu T and Lobie PE: 14-3-3σ mediates G2-M arrest produced by 5-aza-2'-deoxycytidine and possesses a tumor suppressor role in endometrial carcinoma cells. Gynecol Oncol 127: 231-240, 2012.

28. Thangapandiyan S, Ramesh M, Hema T, Miltonprabu S, Uddin MS, Nandhini V and Bavithra Jothi G: Sulforaphane potentially ameliorates arsenic induced hepatotoxicity in albino Wistar rats: Implication of PI3K/Akt/Nrf2 signaling pathway. Cell Physiol Biochem 52: 1203-1222, 2019.
29. Yang Y, Xue K, Li Z, Zheng W, Dong W, Song J, Sun S, Ma T and Li W: c-Myc regulates the CDK1/cyclin B1 dependentG2/M cell cycle progression by histone H4 acetylation in Raji cells. Int J Mol Med 41: 3366-3378, 2018.
30. Wang J, Chang L, Lai X, Li X, Wang Z, Huang Z, Huang J and Zhang G: Tetrandrine enhances radiosensitivity through the CDC25C/CDK1/cyclin B1 pathway in nasopharyngeal carcinoma cells. Cell Cycle 17: 671-680, 2018.
31. Jang SH, Kim AR, Park NH, Park JW and Han IS: DRG2 regulates G2/M progression via the cyclin B1-cdk1 Complex. Mol Cells 39: 699-704, 2016.
32. Fang Y, Yu H, Liang X, Xu J and Cai X: Chk1-induced CCNB1 overexpression promotes cell proliferation and tumor growth in human colorectal cancer. Cancer Biol Ther 15: 1268-1279, 2014.
33. Li Y, Chen YL, Xie YT, Zheng LY, Han JY, Wang H, Tian XX and Fang WG: Association study of germline variants in CCNB1 and CDK1 with breast cancer susceptibility, progression, and survival among Chinese Han women. PLoS One 8: e84489, 2013.
34. Song GQ and Zhao Y: MicroRNA-211, a direct negative regulator of CDC25B expression, inhibits triple-negative breast cancer cells' growth and migration. Tumour Biol 36: 5001-5009, 2015.
35. Sun Q, Shi R, Wang X, Li D, Wu H and Ren B: Overexpression of ZIC5 promotes proliferation in non-small cell lung cancer. Biochem Biophys Res Commun 479: 502-509, 2016.
36. Shi Q, Wang W, Jia Z, Chen P, Ma K and Zhou C: ISL1, a novel regulator of CCNB1, CCNB2 and c-MYC genes, promotes gastric cancer cell proliferation and tumor growth. Oncotarget 7: 36489-36500, 2016.